variation in β.

[23]This theoretical value $B \approx 10^{-10}$ cm^3/sec, which is based on $m_e^* \approx m_h^* \approx m$ (following SD), would be increased by use of $m_e^* \approx \frac{1}{3} m$: this would lower the values m^* Eq. (18) (which is an average over conduction and valence band masses), and hence K, resulting in a higher transition probability (note that $B \propto K^{-10}$!). However, the SD approach gives best agreement with the m^* approach for $F_{ac} \approx 0.5$ (Sec. III B). Use of the m^* method with a lower value of F_{ac} would again lower the transition probability, and agreement with the experimental values could again be obtained.

PHYSICAL REVIEW B VOLUME 7, NUMBER 8 15 APRIL 1973

Far-Ultraviolet Reflectance of II-VI Compounds and Correlation with the Penn-Phillips Gap*

John L. Freeouf†‡
Department of Physics, The University of Chicago, Chicago, Illinois 60637
(Received 15 September 1972)

Synchrotron radiation and standard light sources have been used to measure the polarization-dependent reflectance spectra of BeO, ZnO, ZnS, ZnSe, ZnTe, MgO, CdO, CdS, CdSe, and CdTe for photon energies $0.6 < \hbar\omega < 30$ eV at temperatures $90 < T < 400$ K. The reflectance was analyzed via the Kramers–Kronig relations. We report curves for ϵ_1, ϵ_2, $-\mathrm{Im}(1/\epsilon)$, and $N_{\mathrm{eff}}(\hbar\omega)$ for all of the II*B*-VI compounds studied. Strong structures in the valence-band transition region of the zinc compounds and of the cadmium compounds were found to scale linearly with the Penn–Phillips average energy gap. Reflectance structures corresponding to core excitations were observed. A doublet at about 13.5 eV in CdS, CdSe, and CdTe was identified as a spin-orbit-split transition from the Cd 4*d* level. The observed spin-orbit splitting of this level was 0.6 eV. A shoulder on the low-energy side of this doublet in CdTe at 12.8 eV is identified as originating in the Te 5*s* band.

I. INTRODUCTION

In the past 15 years, measurements of the fundamental absorption spectra of solids have become an increasingly important tool in the study of the electronic configuration of crystals.[1,2] Most research, however, has been limited to wavelengths above 1050 Å (below about 12 eV), where LiF windows and hydrogen discharge tubes can be used. Above 12 eV continuous discharge sources are quite weak, while line sources limit the available resolution.[3] Further, low-temperature reflectance measurements require high vacuum (10^{-8} Torr) to avoid surface contamination. This vacuum requirement is difficult to achieve above 12 eV, where no windows can be used to separate the light source from the sample since no solids transmit light of energies larger than 12 eV. Finally, polarized light is useful when studying anisotropic materials; no transmission polarizer is possible above 12 eV, and reflection polarizers involve large signal losses because of the low reflectance magnitudes of all materials at such high energies.

The use of synchrotron radiation sources has removed these difficulties.[4] It provides an intense polarized continuum spectrum of light throughout the vacuum-ultraviolet spectral region. Further, in contrast to gas-discharge sources, the synchrotron source itself is maintained at ultrahigh vacuum (10^{-9} Torr), thus obviating the need to isolate the sample from the light source when performing low-temperature measurements.[4]

We use synchrotron radiation from the 240-MeV electron storage ring at the University of Wisconsin Physical Science Laboratory.[5] This source is at least two orders of magnitude more intense than conventional gas-discharge sources at energies $E > 12$ eV. Further, the light at our sample is more than 80% polarized. It therefore facilitates the study of the optical properties of anisotropic materials at energies well above 12 eV. A tungsten lamp and reflection polarizer were used in the energy range 0.6–4.5 eV.

The II-VI compounds are of great intrinsic interest. In particular, they provide us with core states accessible to our measurements; the Zn 3*d* and Cd 4*d* states are 8–10 eV below the valence band.[6] Band-structure calculations have had difficulty in locating these states precisely, particularly in the oxides.[7,8] It is hoped that the data presented here will help to resolve this problem. (A preliminary account of this work has been presented elsewhere.[9]) Further, the valence *s* shell of the group-VI atoms lies within our energy range; its energy position has been calculated,[10,11] but until recently not observed in these materials. These *s* bands should provide a sensitive test of the hybridization of the *s* and *p* orbitals of the group-VI atom and therefore increase our knowledge of the chemical bonding of these materials.

These materials are all chemically related. The valence shells of group-IIA and -IIB and of the

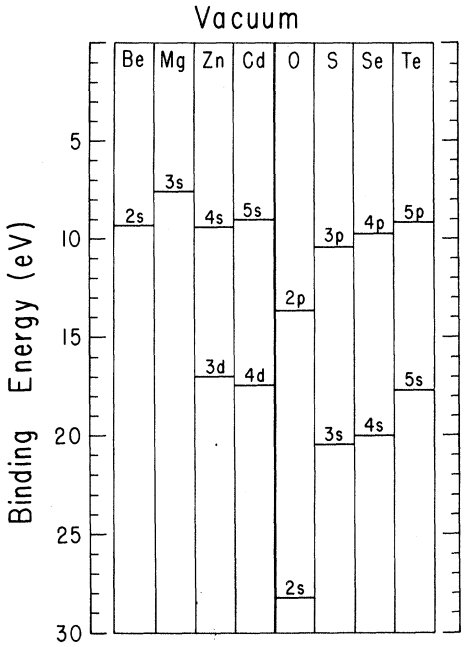

FIG. 1. Atomic energy eigenvalues for the atomic components of the II-VI compounds reported in the present work.

group-VI atoms are identical except for different principal quantum numbers. Also, the IIB atoms have filled d shells at energies close to the energies of their valence shells. In view of these chemical similarities, we searched for a scaling parameter for the energies of strong structures. It was found that the energies of strong structures scaled linearly with the Penn–Phillips[12,13] energy gap, if we stayed within the series of a single metal. This correlation has been used in interpreting the spectra, particularly for materials for which density-of-states calculations have not been performed.

This paper reports measurements of the near-normal-incidence reflectance spectra of BeO, ZnO, ZnS, ZnSe, ZnTe, MgO, CdO, CdS, CdSe, and CdTe in the energy range 0.6–25 eV and at temperatures $100 < T < 400$ K. These results extend the energy range at which the optical properties are known and further extend the energy range for which low-temperature results have been obtained. Although all of these materials have been studied before at energies below 12 eV,[14–16] and in many instances at low temperature,[17–27] experimental work above 12 eV has been more limited.[26–34] Reflectance measurements with polarized light above 12 eV have been performed only on ZnO.[33] No low-temperature data above 10 eV have been reported for these materials. The measurements reported here reveal more structure than had previously been observed, and these new structures are exploited in the study of these materials.

A brief discussion of the chemical considerations and current band-structure calculations is presented in Sec. II. The experimental techniques are presented in Sec. III and an overview of the results is given in Sec. IV. Section V discusses the observed core-state transitions. Section VI presents a discussion of the temperature and polarization dependence of the individual crystals, as well as a comparison with density-of-states calculations when available. Section VII presents the results of a Kramers–Kronig analysis of these measurements.

II. THEORETICAL CONSIDERATIONS

The materials examined here are closely related chemically. The metal atoms all have an outer filled s shell, an empty p shell, and the group-IIB atoms have a filled d shell about 10 eV below the filled s shell. The group-VI atoms have a filled s shell and four electrons in their outer p shell. No other electrons in the atoms lie at energies accessible to our measurements.

A graph of atomic energy levels is shown in Fig. 1. All levels are referred to vacuum.[35] One notes that the greatest energy difference between the valence electrons of the metal (outer s shell) and the group-VI atom (outer p shell) is in CdO and MgO. The energy difference between the d shell of the metal and the p shell of the group-VI atom has been used as a first approximation to the separation of the d band and valence band in the solid.[7] This ignores the possibly large energy shift caused by a transfer of charge from the metal atom of the group-VI atom.[36] Such a charge transfer would bind the d electrons more tightly to the metal atom. It would become larger as the p shell of the group-VI atom becomes more tightly bound, and hence closer in energy to the uncorrected d shell of the metal. The charge transfer will therefore be smallest in the tellurides, as the energy difference between the s shell of the metal and the p shell of the tellurium is quite small. It is interesting that in this case the s shell of the tellurium has an energy quite similar to that of the d shell of the metals. This fact will be of assistance in locating transitions from the s shell of tellurium, and perhaps the other chalcogens, to the conduction band.

The bonding of these materials is perhaps best discussed in terms of their crystal structures. To this end we divide the crystals into two types—fourfold- and sixfold-coordinated structures.

The sixfold compounds are CdO and MgO; they are highly ionic and involve a transfer of the s electrons of the metal to fill the p shell of the oxygen. This produces positive (metal) and nega-

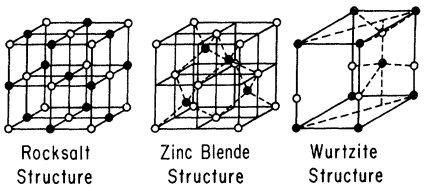

FIG. 2. Structures of the crystals studied in the present work.

tive (oxygen) ions, the latter with a p-like outer electron shell. The metal ion has either a p-like outer shell (MgO) or a d-like outer shell (CdO). The p shell of Mg is too tightly bound (55 eV) to be observed in this experiment, but the d shell of CdO, while perhaps more tightly bound in the ion than in the atom, should still lie well within our energy range. The first and second conduction bands come, to a first approximation, from the unfilled s and p shells of the metal ion.

The fourfold-coordinated compounds are still highly ionic.[13] Their bonding involves some hybridization of the s and p orbitals of both atoms, but still results in a large localization of charge about the group-VI atom.[37] The hybridization, however, makes it difficult to speak of atomiclike orbitals. For instance, the first conduction band of these materials has a large concentration at the site of the group-VI atom[37] and has almost no density of states at the metal site, in contrast to the more ionic case where there is a large concentration at the metal site.[38] The valence band, however, is still largely characteristic of the group-VI atom.[37]

Although these materials are chemically similar, they exist in two crystal structures—zinc blende (ZB) and wurtzite (WU). One might expect that the different Brillouin zones associated with these two crystal structures would lead to significantly different spectra. It is observed, however, that these materials (except the oxides) have quite similar spectra. Let us see if a close examination of these crystal structures will explain this observation.

Figure 2 shows the WU and ZB crystal structures. Note that they are actually quite similar; they both have four nearest neighbors for each atom, and twelve next-nearest neighbors.[39] The four nearest neighbors occupy identical positions about the reference atom in either structure, but they are equivalent by crystal symmetry in the ZB lattice and nonequivalent in the WU lattice. Of the twelve next-nearest neighbors, only three occupy different positions in WU than in ZB. The effects of this close similarity in lattice structure upon the Brillouin zones (BZ) of the structures has been examined in some detail.[39] It was found that if one aligns two WU BZ's along the Γ-A axis, then one Γ-L axis of the ZB BZ is mathematically equivalent to the Γ-A-Γ' axis in the WU zone[39] (see Fig. 3). In the reduced zone scheme this is simply a "folding back" of the axis upon itself. It was also found that other Γ-L axes of the ZB BZ mapped onto part of the Γ-U ($\frac{2}{3}$) axis, although other parts of the ZB BZ also map onto this axis.[40]

We can therefore conclude that a transition along the Γ-A axis of the WU zone should have an equivalent transition along the Γ-L axis of the ZB BZ. Also, a transition along the Γ-L axis of the ZB BZ should have equivalent transitions along the Γ-A axis and along the Γ-U ($\frac{2}{3}$) axis, both of the WU BZ.

A more phenomenological approach was pursued by Bergstresser and Cohen.[40] They calculated the band structure (BS) for ZnS in both the ZB and WU structures. They calculated ϵ_2 by means of density-of-states calculations from both band structures and tried to deduce from these results which parts of the WU BZ gave rise to peaks corresponding to those from the ZB BZ. They agreed with the above conclusions and made some further deductions. They found that the ZB points X, K, and U are mapped primarily onto two portions of the WU BZ. The first portion of the zone is a region around M and along the Σ axis, and the second is a region around K and along the z direction.[40]

MgO and CdO crystallize in the rocksalt structure which is sixfold coordinated. This structure has the same BZ as does the ZB structure.[41] We can therefore connect regions of the ZB and rocksalt Brillouin zones. However, some caution is required as the symmetry groups involved are the same only at some portions of the Brillouin zone (i.e., Λ).[41,42]

Table I provides a brief summary of the materials studied. It lists the crystal structure of the materials reported in this paper, the coordination number, the Brillouin zone associated with this crystal structure, and the Penn–Phillips energy gap, which is an average energy gap for valence-band to conduction-band transitions.

Since these crystals encompass three different

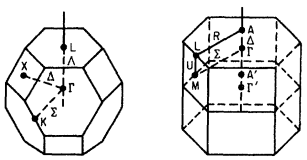

FIG. 3. Brillouin zones of the crystals studied in the present work. Two WU zones are shown aligned as discussed in the text.

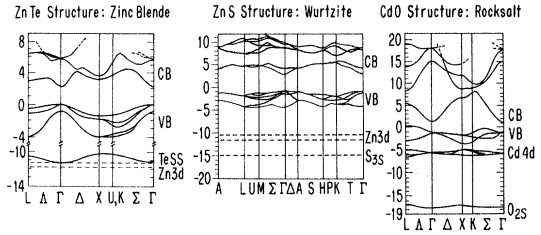

FIG. 4. Band structure for ZnTe (Ref. 24), ZnS (Ref. 7), and CdO (Ref. 45). We have indicated the approximate location of outer core states when necessary.

crystal structures, we shall discuss the BS of each structure separately. We shall, however, first make some comments of general applicability to all group-IIB-VI materials discussed here.

The filled [valence-band (VB)] states may be divided into four regions. The first region is the deep core states, 30 eV or more below the conduction band, and hence not accessible to observation with our apparatus. The second region lies 10–30 eV[10,11,24,25,43,44] below the conduction band and derived from the outer filled s shell of the group-VI atom. This has been shown by BS calculations to remain strongly s like and localized at the site of the group-VI atom.[37] The third region lies 10–20 eV below the conduction band and may overlap the s states in some cases. This is the filled d band of the metal atom.[7,44,45] The fourth region is the upper valence band. It is mostly p like with some s character and is still apparently strongly centered upon the group-VI atom.[37]

Figure 4 shows a BS for the ZB crystal structure,[24] including spin-orbit (SO) effects. The upper VB is SO split at Γ into two levels, Γ_8^- and Γ_7^-, which correspond to $j=\frac{3}{2}$ and $j=\frac{1}{2}$, respectively. Away from Γ, the line coming from Γ_8^- is no longer pure $j=\frac{3}{2}$, and so this level is SO split into $L_{4,5}$ and L_6.

The SO-split d levels are drawn flat, as the details of their k dependence has not yet been calculated (it is expected to be small, as they do not participate strongly in the bonding). The lowest VB is about 2 eV wide and is the s-like band of the group-VI atom.

Figure 4 shows a BS[7] for the WU crystal structure neglecting the effects of the SO interaction. Again the three regions of the VB are clearly separated.

Figure 4 also shows a BS for CdO (rocksalt structure) as calculated by Maschke and Rössler.[45] We have added the lowest s state at its atomic energy. Note that the VB maxima are well away from Γ and much higher than at Γ; this is due to the large mixing of VB states and d-band states in these portions of the zone, a result of the small separation between the VB and the d bands resulting from this calculation. The position of the d band in CdO has been measured by x-ray photoemission,[46] which locates it at about 3 eV further below the VB than this BS calculation indicates. This increase in energy separation will decrease the mixing of valence and d states, and hence bring the off-Γ maxima to lower energies.

Pseudopotential BS calculations have been used as the starting point for joint density-of-states calculations of ϵ_2 and of the reflectance of these materials.[14,23–25,43] The results of these calculations imply that peaks in the reflectance are usually caused by peaks in the joint density of states from a region of the BZ, and while these peaks may be associated with a critical point, they occur at a somewhat different energy than that of the critical point itself.

III. EXPERIMENTAL PROCEDURE

The apparatus used for these measurements has been reported in detail elsewhere.[4] We shall therefore only outline the method used. Synchrotron radiation from the 240-MeV electron storage ring at the University of Wisconsin was used as a continuous source of polarized radiation in the photon energy range 4–30 eV. A standard source was used in the energy range 0.6–4.5 eV. The reflectance in both cases was measured by the rotating-light-pipe scanning-reflectometer technique,[47] permitting the reflectance to be measured directly during the wavelength scan. Reported reflectance magnitudes for photon energies greater than 8 eV disagree significantly with one another. Differences in surface quality may explain some of the experimental scatter. However, in some instances the reported magnitudes disagree by nearly a factor of 2 without significant alteration of the relative spectral shapes. This implies a systematic error; let us therefore search for possible systematic errors in the magnitudes determined by our system.

To determine absolute reflectance magnitudes one must accurately measure the light incident on the sample and also measure the light reflected from the sample. In both of these measurements

TABLE I. Properties of the crystals studied.

Material	Structure	Coordination no.	Brillouin zone	Penn–Phillips gap (eV)
BeO	WU	4	B	18.1
MgO	rocksalt	6	A	14.5
ZnO	WU	4	B	11.8
ZnS	WU	4	B	7.8
ZnSe	ZB	4	A	7.05
ZnTe	ZB	4	A	5.8
CdO	rocksalt	6	A	10.3
CdS	W U	4	B	7.14
CdSe	WU	4	B	6.6
CdTe	ZB	4	A	5.4

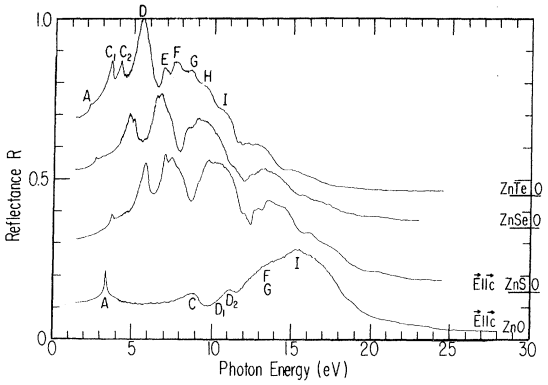

FIG. 5. Reflectance spectra of zinc compounds at 300 K. Curves are vertically shifted as indicated to prevent overlap.

one must capture the full light beam. As our detector is smaller (about 4 mm in diam) than most detectors used in such measurements, extra care is required in meeting this requirement. We placed a sodium-salicylate-coated screen at the position of the light pipe and photographed the fluorescence from first-order light at three wavelengths (600, 1650, and 2700 Å) representative of our entire spectral region. The beam is trapezoidal; the largest dimension of the beam at the detector is 2.4 mm, which is easily captured by our 4-mm light pipe.

The detector surface has a nonuniform response. One must therefore capture the reflected beam on the same portions of the detector as captured the incident light. In our system the light is focused on the sample. As the detector measures both the incident and the reflected light at the same distance from the sample, the light beam is therefore of the same size and shape.

Our magnitudes are generally higher than those reported elsewhere. If we are in error, this implies that we capture a smaller portion of the incident beam than of the reflected beam, or that the detector response is smaller for the incident than for the reflected beam. Let us see what evidence we have for such errors.

We have measured the reflectance spectra of CdTe on four occasions over a period of five months. We have measured ZnO $\vec{E} \perp \vec{c}$ twice, with a time separation of six months. During the intervening period we have changed the grating, light pipe, and photomultiplier tube and recoated the focusing mirror with gold and the light pipe with sodium salycilate; the maximum scatter of reflectance magnitudes for CdTe was $\Delta R = 0.03$ (for $R = 0.4$ at 8 eV), while the maximum scatter for ZnO was $\Delta R = 0.02$ (for $R = 0.3$ at 15 eV). Any errors due to nonuniform detector response or not capturing all of the incident light beam should have been affected by these changes in our system; the small scatter implies that these errors are also small. We estimate that our absolute magnitudes are correct to within $\Delta R = \pm 0.03$. Further evidence in support of our magnitudes will be presented in the section dealing with the results of a Kramers–Kronig analysis of our measurements (Sec. VII).

Single crystals of ZnO, ZnS, ZnSe, ZnTe, MgO, CdSe, and CdTe were cleaved just prior to mounting in the experimental system. Samples of BeO, CdO, and CdS were found with well-developed natural surfaces. They were rinsed in fresh methanol and blown dry just prior to mounting in the experimental chambers. The sample of CdO measured in the high-energy region had a slightly curved face, so the absolute magnitudes reported for it are less certain than for the other materials. A flat sample was measured in the low-energy region, and the high-energy values were scaled to match these results. The scale factor used was ~1.4.

IV. GENERAL TRENDS AND PENN-PHILLIPS GAP

The room-temperature near-normal-incidence reflectance spectra of ZnO, ZnS, ZnSe, and ZnTe are presented in Fig. 5, and the spectra of CdO, CdS, CdSe, and CdTe are shown in Fig. 6. The curves have been zero shifted as indicated to prevent overlap.

The positions and shapes of reflectance peaks are the primary direct means of relating spectra to the electronic configurations of materials. The most striking characteristic of all of the chalcogenides is that the reflectance is fairly large and structured in an energy range from the fundamental absorption edge to about 11 eV; the reflectance then decreases sharply, and more structure then appears at this lower magnitude.

This sharp decrease in reflectance magnitude is taken as an indication that the oscillator strength of valence-band to conduction-band transitions has been nearly exhausted. The higher-energy peaks

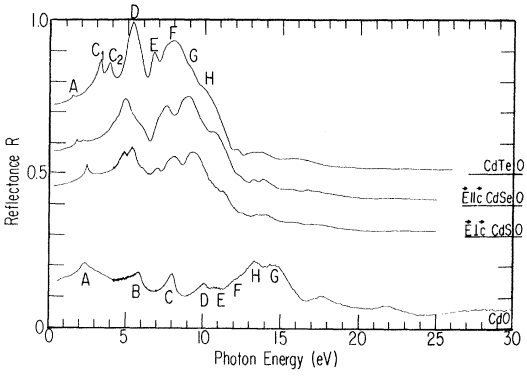

FIG. 6. Same as Fig. 5 for cadmium compounds.

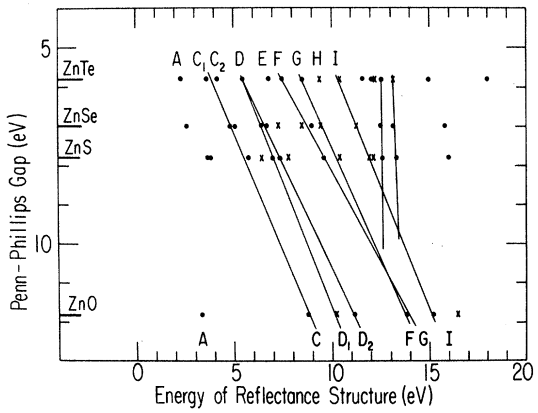

FIG. 7. Energies of reflectance structures (horizontal) vs Penn–Phillips average energy gap (vertical for the zinc compounds.

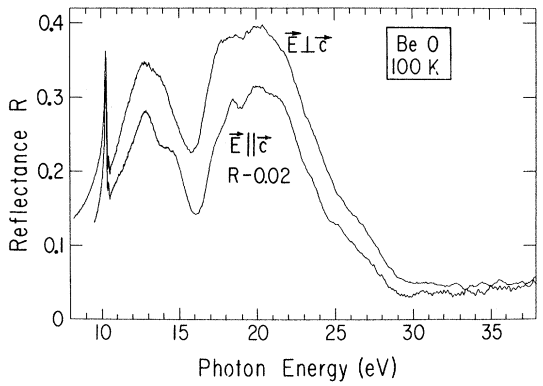

FIG. 9. Reflectance spectra of BeO at 100 K for $\vec{E} \perp \vec{c}$ and $\vec{E} \parallel \vec{c}$. The curve for $\vec{E} \parallel \vec{c}$ has been shifted down by $RS = 0.021$ to prevent overlap.

are therefore believed to correspond to a different set of interband transitions—originating in the metal atoms's outer *d* core or the chalcogen's valence *s* band. Both bands are probably involved in the absorption in this region.

Figures 7 and 8 show a more detailed means of relating these spectra to the electronic configurations of the solids studied. It was found that if one plots the energies of strong structures in the reflectance spectra of these materials against the Penn–Phillips energy gap,[12,13] one obtains straight lines connecting structures occupying similar positions in similar spectra. It was further found that within the energy range in which available BS calculations are accurate, and where regions of the BZ can be directly compared, these lines connect peaks due to essentially equivalent interband transitions. This provides a powerful tool in the interpretation of these spectra, since one can then use a BS calculation upon one crystal to directly interpret the spectrum of another material of the same structure. It may also be used to compare the origin of an interband transition in the Brillouin zones of two different crystal structures.

We note that in Figs. 7 and 8, the slopes of the lines change sharply at the region earlier defined as the end of the upper VB transitions and the beginning of *d*-band or outer *s*-band transitions. This provides a more satisfactory method of determining the onset of deeper VB transitions. Note further than in the oxides there are very strong peaks in the energy range 13–15 eV. These were assigned by other workers[33] to *d* transitions because their energy is similar to that of *d* transitions in the chalcogenides, although the oscillator strength associated with these peaks is much greater than that associated with the known *d* transitions in the chalcogenides. Our correlation demonstrates that these peaks result from upper VB to conduction-band transitions, although *d*-band transitions may also take place in this energy range. This conclusion is further supported by the spectra of BeO and MgO, shown in Figs. 9 and 10. BeO is hexagonal, as is ZnO, and MgO and CdO

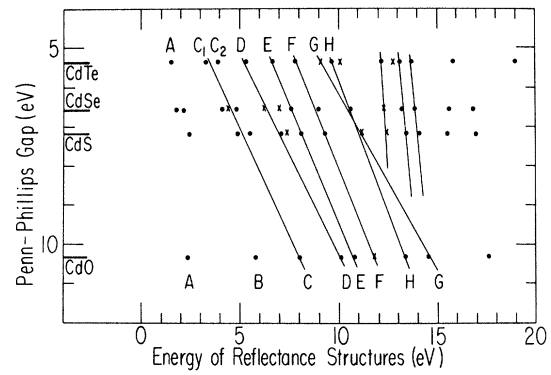

FIG. 8. Same as Fig. 7 for cadmium compounds.

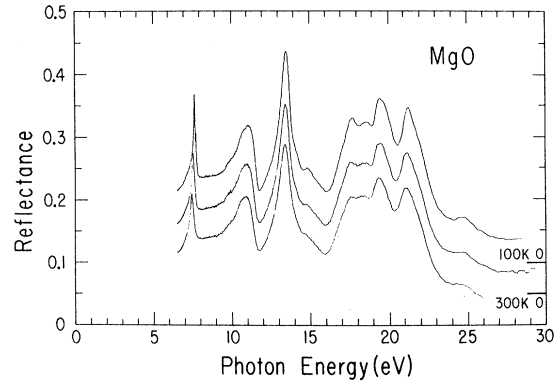

FIG. 10. Reflectance spectra of MgO. Vertical shifts of $+RS$ and $+2RS$ separate the 300- and 100-K curves from the curve obtained at 400 K (lowest curve). $RS = 0.05$.

are both in the NaCl structure. In all of these materials strong absorption takes place at energies 10–15 eV above the fundamental absorption edge. It should be noted that MgO and BeO have no core states (except the outer s shell of the oxygen) accessible to measurements in our energy range.

We shall discuss the first structure above the fundamental absorption edge. In the zinc series this provides a simple illustration of the procedures followed. We note that the peaks labeled "C" occupy similar portions of the spectra in all of the materials. We further note that their energies vary almost linearly with the Penn–Phillips energy gap (using a weighted average of C_1 and C_2 in the selenide and telluride, as they are a SO-split doublet). We then look at BS and density-of-states calculations.[11,23,24,44,48] For ZnTe we find that the peaks C_1 and C_2 are a SO-split doublet from the Λ axis of this ZB material; a similar result holds for ZnSe. In ZnS two differences occur[7,40]; the SO splitting of the upper VB (due to the group-VI atom) is too small to observe, and the crystal structure has changed to wurtzite. The first change implies only one peak; the second change could cause this peak to become two peaks as the Λ axis of the ZB BZ goes to nonequivalent portions of the WU BZ as discussed earlier. We see only one peak in ZnS. Density-of-states calculations[40] upon hexagonal ZnS imply that this peak does indeed come from the Γ-A axis and the U axis of the WU zone, the two portions of this zone related to the Λ axis of the ZB Brillouin zone. The same areas of the zone have the correct energy for the observed peak in ZnO according to the only BS calculation upon this material known to the author.

In the cadmium series the same discussion is valid for the telluride.[25,48,49] The selenide, however, crystallizes in the WU crystal structure, leading to a more complicated spectrum. Here one finds three "C" peaks, not two. This is due to two effects. The hexagonal crystal field has in this case removed the degeneracy of the Γ-A axis and the U region of the zone.[28,40] As we saw, this did not happen in the zinc series. The second effect is related to the first; the region around U in the wurtzite lattice has selection rules against one of the SO-split components. In CdS one sees only two peaks. The crystal-field splitting is still evident, but the SO splitting is not too small to be observed.

We now come to CdO, for which only one BS calculation is known to the author.[45] This calculation implies that the peak labeled C in CdO results from transitions between the second highest valence band and the lowest conduction band at L (for the rocksalt BZ), or from the highest valence band and the second lowest conduction band at the same point. All other peaks labeled C in this series result from transitions between the highest valence band and the lowest conduction band. As noted in Sec. III, the BS under discussion may be in error at this portion of the BZ. If the mixing of the d band with this valence band is reduced, the effect would be to lower the energy of the highest VB at L. This would bring the BS into closer agreement with our tentative assignment of this peak as a highest-valence-band to lowest-conduction-band transition at L.

CdO and MgO are both in the rocksalt structure. Their spectral shape is nearly identical for the first three reflectance peaks. In both MgO and CdO the first peak above the band gap is theoretically assigned to transitions at L between the highest valence band and the lowest conduction band.[43,45] A density-of-states calculation has been performed[43] for MgO; the strength of this peak cannot be explained by density of states, even considering matrix elements. This peak is not yet understood.

The association of peaks with the same interband transitions in different materials may be experimentally tested by the study of the spectra of mixed crystals. The only such study on materials within a series known to the author was performed by Hengehold and Fraime[50] on $CdS_{1-x}Se_x$. The associations reported here match those observed in that experiment. Hengehold and Fraime further observed that the energies of most peaks varied in an approximately linear fashion with composition. The largest departure from linearity occurred at the peaks labeled C in our graphs.

Another possibility lies in going between the two series. One such experiment[51] considered $Cd_{1-x}Zn_xS$. Unfortunately, a discontinuity of some structures was found at $x = 0.92$; this made it difficult to associate peaks in the two materials by this method, as they could not be followed continuously from one material to the other.[51]

Our scaling law works quite well within a series. If one goes between series it is not quite as accurate, although it still defines an energy range for valence-band to conduction-band transitions. We have also applied this technique to the series BeO, MgO, ZnO, and CdO. This series contains two crystals in the rocksalt structure and two crystals in the hexagonal structure. Although the peaks are too ill defined for following specific transitions, the general energy range for valence-band to conduction-band transitions still follows this scaling law.

V. CORE EXCITATIONS

Figure 11 shows the high-energy portion of the reflectance spectra for the cadmium compounds. The curves have been zero shifted as indicated to prevent overlap. All of these spectra were measured at 100 K. Note that there is a doublet at

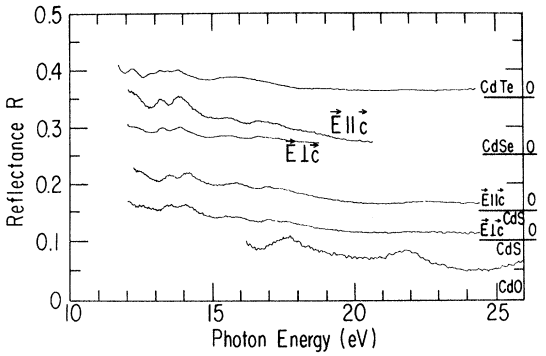

FIG. 11. Reflectance spectra of the cadmium compounds in the core excitation region measured at 100 K.

about 13.5 eV in all three chalcogenides. This doublet is split by about 0.6 eV. The fact that its energy does not change upon going from the sulfide to the telluride implies that it is intrinsic to the cadmium atom. The SO splitting of the Cd 4*d* in the free atom is about 0.7 eV.[52] Photoemission results[46,53–56] indicate that the Cd 4*d* band is located about 10 eV below the top of the VB in these materials. Band-structure calculations[25,44,49] for these materials show only one region within 5 eV of the top of the VB which has a large density of states and is of *p*-like symmetry with respect to the metal atom. This is the lowest suitable final state for a transition from the *d* states of the atom. This region is around X_1 in the ZB lattice and lies about 3.5 eV above the top of the VB. This doublet can therefore be identified as a *d*-band to conduction-band transition at X_1, in agreement with BS calculations and photoemission results.

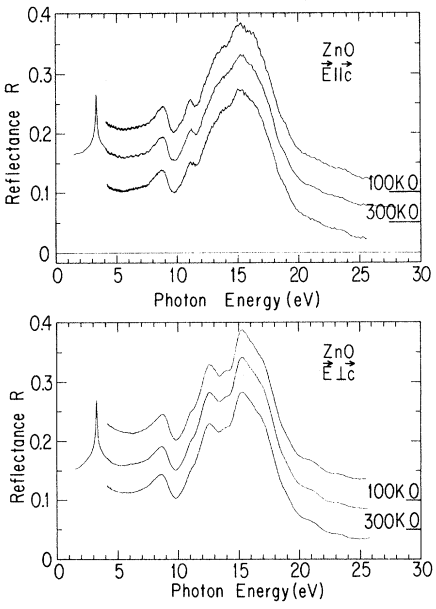

FIG. 12. Reflectance spectra of ZnO $\vec{E}\perp\vec{c}$ and $\vec{E}\parallel\vec{c}$. $RS=0.05$.

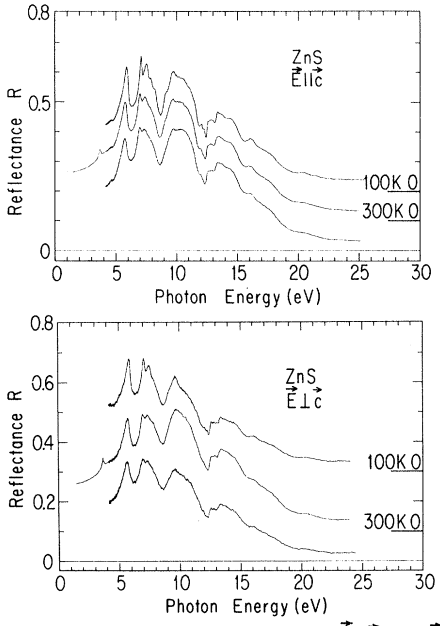

FIG. 13. Reflectance spectra of ZnS $\vec{E}\perp\vec{c}$ and $\vec{E}\parallel\vec{c}$, $RS=0.1$. The 100-K curve for $\vec{E}\perp\vec{c}$ was shifted by $3RS$ because the surface was contaminated.

In the zinc compounds, one does not observe a well-defined doublet. This may be understood when one considers that the SO splitting of the zinc 3*d* states in the free atom[57] is only 0.4 eV. The width of the components of the doublet in the cadmium series would greatly smear such a small splitting. However, there is a steplike structure at about 12.5 eV in the zinc chalcogenides that is probably the Zn-3*d*–band to conduction-band transition in these materials.

CdTe has a shoulder on the low-energy side of its *d*-band doublet. It was mentioned in Sec. III that the atomic energy levels of the Cd 4*d* and of the Te 5*s* lie at nearly the same energy, and little charge transfer between these two atoms would be expected. Preliminary photoemission results on

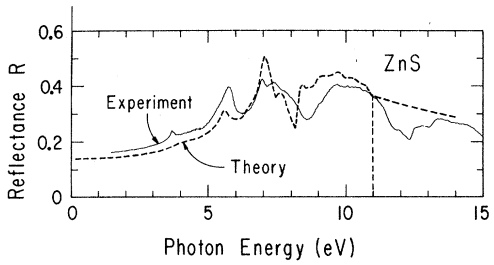

FIG. 14. Solid curve is our 300-K reflectance for ZnS. The dotted curve is reflectance calculated from a pseudopotential BS (Ref. 11).

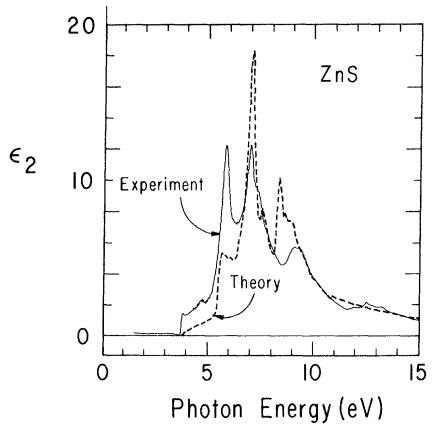

FIG. 15. Solid curve is the ϵ_2 obtained by Kramers–Kronig analysis of our 300-K reflectance spectra for ZnS. Dotted curve is ϵ_2 calculated from a pseudopotential BS (Ref. 11).

CdTe by Eastman[58] show that this shoulder is in the filled states. We therefore believe that this shoulder is due to a transition from the tellurium 5*s* filled valence shell to a low-lying conduction-band state. The final state in this case is probably in the X_3 conduction-band region, as this band is of *p*-like symmetry with respect to the chalcogen.

The other high-energy structures do not have such well-defined interpretations. We may note that the atomic energy levels of the outer filled *s* shells of sulfur and selenium are about 10 eV below their outer *p* shell (or valence shell), while the corresponding energy difference[6] for tellurium is about 8 eV. We therefore expect S-3*s*– and Se-4*s*–band to conduction-band transitions at energies 2 eV above the corresponding Te-5*s* transition. We looked for structures at about 15–16 eV in both the Zn and Cd sulfides and selenides. There are indeed such structures. In fact, in the (hexagonal) CdS and CdSe there are two such structures, perhaps crystal-field split. Performing a similar

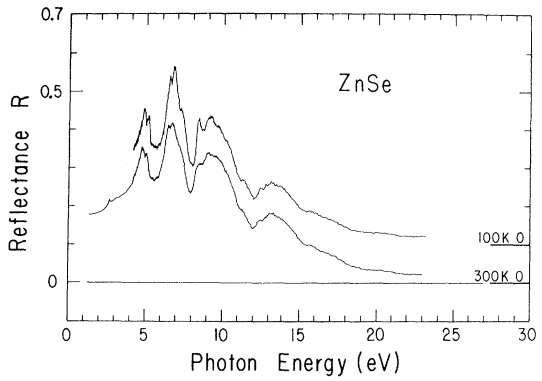

FIG. 16. Reflectance spectra of ZnSe at 300 and 100 K, $RS = 0.1$.

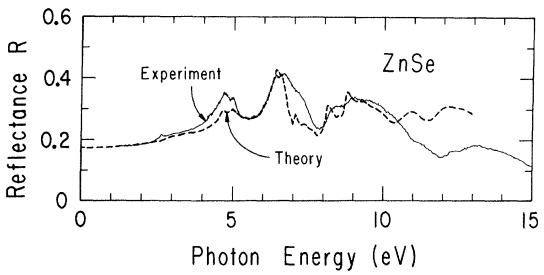

FIG. 17. Same as Fig. 14 for ZnSe. The theoretical curve is from Ref. 24.

analysis on the oxides, one concludes that the oxygen-2*s*–band to conduction-band transition should occur at about 21–22 eV; such structures can be found for both ZnO and CdO. However, there is also a slight structure at 22 eV in CdS, and the oxides have structures at about 16–17 eV. We therefore conclude that assignments of these higher-energy peaks to transitions from the outer *s* shell of the group-VI atom are highly speculative. Photoemission measurements of these *s* states would be of great assistance in understanding these structures.

VI. DISCUSSION OF INDIVIDUAL SPECTRA

The temperature and polarization dependence of the reflectance spectra of the zinc and cadmium compounds studied are shown in Figs. 12–25. To separate the curves corresponding to different sample temperatures, the room- and low-temperature curves have been shifted vertically by an amount *RS* and 2*RS*, respectively, so that the curves for 100 K are highest, and the curves for 400 K are lowest. The 300-K measurement extends from 0.6 to 30 eV; the 100- and 400-K measurements were limited by our experimental apparatus to the energy range 4–30 eV. All curves have been corrected for the effects of second-

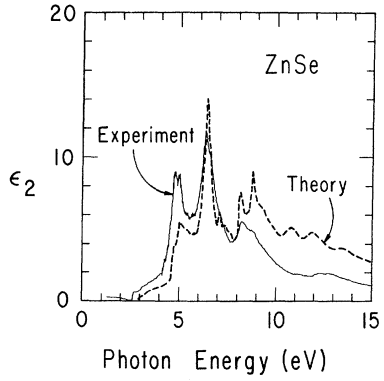

FIG. 18. Same as Fig. 15 for ZnSe. The theoretical curve is from Ref. 24.

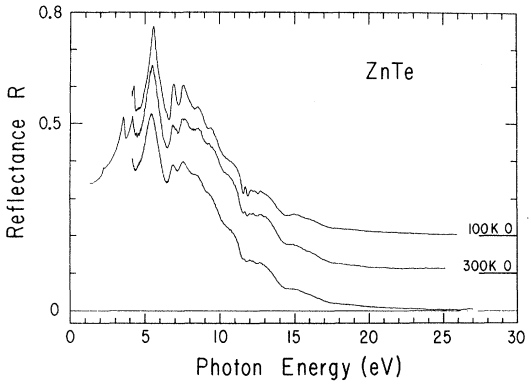

FIG. 19. Reflectance spectra of ZnTe, $RS = 0.1$.

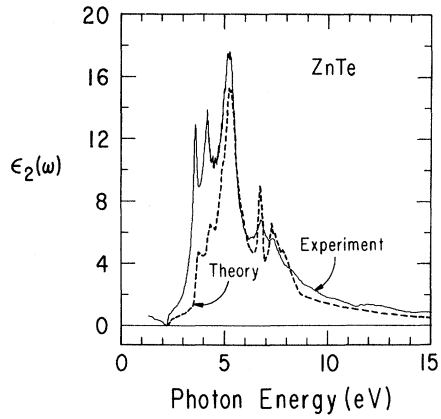

FIG. 21. Same as Fig. 15 for ZnTe. The theoretical curve is from Ref. 24.

order light from our grating. Tables II–IV list the energies of all reflectance structures observed.

Let us briefly discuss the spectra of each material. The temperature-dependent spectra for ZnO $\vec{E} \perp \vec{c}$, $\vec{E} \parallel \vec{c}$ are shown in Fig. 12. Above the band-gap exciton almost no temperature dependence is seen. The band-gap exciton was measured only at room temperature; the temperature dependence of this peak has been studied in great detail by other workers.[33,59,60]

At higher energies, the first structure observed lies at about 8.7 eV and is nearly independent of temperature and polarization. Other workers[32,33] have reported a small structure at about 7 eV, also independent of polarization.[33] We carefully studied this region of the spectrum but saw no such peak, although our relative accuracy of $\Delta R = 0.005$ should have permitted its observation. At higher energies our agreement with reported spectral shape and polarization dependence was quite good, although our reflectance magnitude for the peak at 15 eV is $R = 0.27$, in contrast with the reported value of 0.17.[32,33] The measurements on ZnO $\vec{E} \perp \vec{c}$ were puzzling. The measurements with synchrotron radiation were not self-consistent; one sample gave higher reflectivities at 4 eV than did the other (reflectances were similar for $E > 8$ eV). We have chosen to report the spectra with higher reflectance values because they are in agreement with the results of our highly reproducible low-energy measurements. It should be noted that our low-energy data (for ZnO $\vec{E} \perp \vec{c}$) disagree with previously reported results[33] for energies $E > 3.8$ eV.

Figure 13 shows the temperature-dependent spectra of ZnS for $\vec{E} \perp \vec{c}$ and $\vec{E} \parallel \vec{c}$. The 100-K curve for $\vec{E} \perp \vec{c}$ was obtained from a contaminated sample, causing a decrease in the magnitude of R such that R was depressed more as λ became smaller. As there was little polarization dependence in ZnS we did not remeasure ZnS $\vec{E} \perp \vec{c}$ at 100 K when the source of the contamination was removed. We note that the low-temperature spectra do not reveal more structure, but some shoulders become better defined; in particular, the two shoulders at 12 eV become peaks. The broad structure at 10 eV shows the most dependence upon polarization. The rest is rather independent of polarization. Our agreement with the work of Cardona[28] on this material is excellent. The structures are all in agreement as to shape, and the magnitudes are within $\Delta R = 0.05$.

Cohen and co-workers have computed the BS of most of the materials discussed here using the

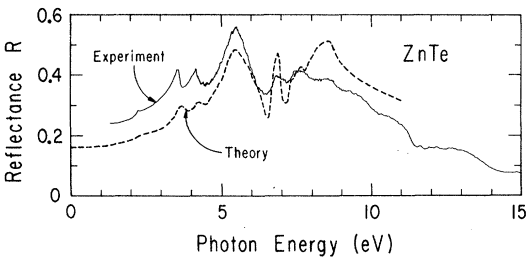

FIG. 20. Same as Fig. 14 for ZnTe. The theoretical curve is from Ref. 24.

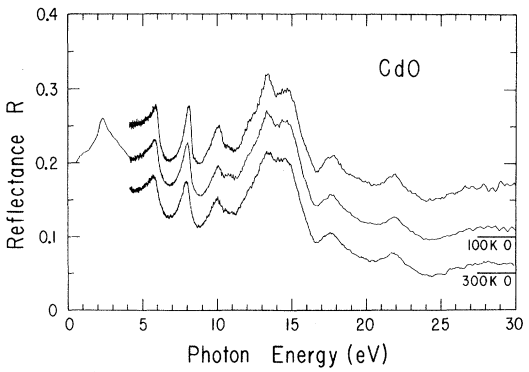

FIG. 22. Reflectance spectra of CdO, $RS = 0.05$.

TABLE II. Energies (in eV) of prominent features in the reflectance spectra of the zinc compounds.

400 K	300 K ZnO $\vec{E} \parallel \vec{c}$	100 K	400 K	300 K ZnO $\vec{E} \perp \vec{c}$	100 K	400 K	300 K ZnS	100 K	400 K	300 K ZnSe	100 K	400 K	300 K ZnTe	100 K
•••	•••	•••	•••	•••	•••	•••	3.698	•••	•••	•••	•••	•••	•••	•••
•••	3.34	•••	•••	3.3	•••	•••	3.76	•••	•••	2.663	•••	•••	2.261	•••
•••	•••	•••	•••	•••	•••	•••	•••	(s)4.6	•••	4.8	4.9	•••	3.587	•••
8.7	8.8	8.8	8.6	8.6	8.75	•••	•••	•••	•••	5.05	5.2	•••	4.166	4.25
•••	•••	•••	•••	•••	•••	5.7	5.75	5.7	•••	6.42	6.55	5.41	5.45	5.55
10.1	10.2(s)	10.2	•••	•••	•••	•••	•••	5.8	•••	6.7	6.8	6.78	6.82	6.9
•••	•••	•••	11.0	11.0	(s)11.0	•••	•••	•••	•••	7.3(s)	7.3	7.42	7.5	7.55
11.2	11.15	11.1	•••	•••	•••	6.3	6.45(s)	6.5(s)	•••	8.5(s)	8.4(P)	8.2	8.5(s)	8.5
•••	•••	•••	12.6	12.5	12.5	•••	•••	•••	•••	9	9.2	9.2	9.4(s)	9.4
13.8	13.8	(s)13.8	14	13.8(s)	13.8	6.95	7.0	7.05	•••	9.5(s)	9.7	10.2	10.4(s)	10.7
15.2	15.2	15.2	15.2	15.2	15.2	7.35	7.35	7.5	•••	11.3	11.35	11.6	11.6	11.62
16.4	16.2(s)	16.2	17	17(s)	17	7.8(s)	7.8	(s)7.95	•••	12.5	12.5	12.05	12.05	12.05
21	21(s)	21	20.5	20.5	20.5	9.0(s)	9.1	9.1	•••	•••	•••	12.25	12.25	12.25
•••	•••	•••	20.9	20.9	20.9	•••	•••	•••	•••	13.1	13.1	12.65	12.65	12.65
23.4	23.5(s)	23.5	23	23	23	9.55	9.6	9.6	•••	15.8	15.8	13.2	13.2(s)	13.2
•••	•••	•••	•••	•••	•••	10.7	10.4(s)	10.5	•••	20.5	20.5	14.9	14.9	14.9
•••	•••	•••	•••	•••	•••	11.9	11.9	12.0	•••	•••	•••	•••	•••	•••
•••	•••	•••	•••	•••	•••	•••	•••	12.25	•••	•••	•••	•••	•••	•••
•••	•••	•••	•••	•••	•••	12.55	12.6	12.6	•••	•••	•••	•••	•••	•••
•••	•••	•••	•••	•••	•••	13.35	13.35	13.4	•••	•••	•••	•••	•••	•••
•••	•••	•••	•••	•••	•••	14.3	14.3	14.4	•••	•••	•••	•••	•••	•••
•••	•••	•••	•••	•••	•••	16.0	16.0(s)	16(P)	•••	•••	•••	•••	•••	•••
•••	•••	•••	•••	•••	•••	•••	17.8	•••	•••	•••	•••	•••	•••	•••
•••	•••	•••	•••	•••	•••	20.2	20.2	20.3	•••	•••	•••	•••	•••	•••

TABLE III. Energies (in eV) of prominent features in the reflectance spectra of the cadmium compounds.

400 K	300 K	100 K	400 K	300 K	100 K	400 K	300 K	100 K	400 K	300 K	100 K	400 K	300 K	100 K	400 K	300 K	100 K
	CdO			CdS $\vec{E}\perp\vec{c}$			CdS $\vec{E}\parallel\vec{c}$			CdSe $\vec{E}\perp\vec{c}$			CdSe $\vec{E}\parallel\vec{c}$			CdTe	
•••	2.37	•••	•••	2.45	•••	•••	2.5	•••	•••	•••	•••	•••	•••	•••	•••	•••	•••
•••	5.8	5.9	4.8	4.88	4.9	4.8(*s*)	4.8(*s*)	4.8	•••	1.775	•••	•••	1.775	•••	•••	1.512	•••
7.9	8	8.1	5.35	5.4	5.5	5.35	5.4	5.5	•••	2.141	•••	•••	2.141	•••	•••	3.32	•••
10.0	10.1	10.1	6.11	6.0(*s*)	6.0	6.2	6.2(*s*)	6.2	•••	4.131	4.2	•••	4.2	(*s*)4.3	•••	3.903	•••
•••	10.8	10.8	7.0	7.1	7.1	•••	7.4(*s*)	7.4(*s*)	4.3	4.45(*s*)	4.5	•••	•••	(*s*)4.5	•••	•••	5.2(*s*)
•••	•••	•••	•••	•••	7.6(*s*)	•••	•••	•••	4.8	4.8	4.95	4.8	4.9	5.0	5.3	5.3	5.45
11.8	11.8(*s*)	12.0(*p*)	•••	•••	•••	•••	•••	•••	5.45	5.4(*s*)	5.6	5.4	5.45(*s*)	5.6	6.7	6.7	6.75
•••	•••	•••	8.0	8.1	8.2	8.0	8.0	8.0	6.2	6.2(*s*)	6.4	6.1	6.1(*s*)	6.2	•••	•••	•••
13.3	13.3	13.4	•••	•••	•••	•••	•••	•••	•••	•••	•••	•••	•••	•••	7.8	7.8	•••
•••	•••	•••	9.25	9.3	9.4	9.4	9.4	9.4	7.2	7.0(*s*)	7.2	7.05	7.05(*s*)	7.2	•••	•••	7.9
14.5	14.5	14.6	•••	•••	•••	•••	•••	•••	7.55	7.6	7.6	7.5	7.6	7.65	9.1	9.1(*s*)	9.2
•••	•••	•••	11.2	11.2(*s*)	11.25	11.3	11.3(*s*)	11.3	•••	•••	8.7	•••	•••	8.7	9.7	9.7(*s*)	9.7
17.5	17.6	17.7	•••	•••	•••	•••	•••	•••	9.0	9.0	•••	8.9	9.0	•••	•••	•••	•••
•••	•••	•••	12.5(*s*)	12.5(*s*)	12.5(*p*)	12.5(*s*)	12.5(*s*)	12.5(*s*)	•••	•••	9.15	•••	•••	9.2	10.2	10.1(*s*)	10.1
21.9	21.9	21.9	•••	•••	•••	•••	•••	•••	10.6(*s*)	10.6(*s*)	10.6(*P*)	10.6(*s*)	10.6(*s*)	10.4(*s*)	12.1	12.15(*s*)	12.1(*P*)
•••	•••	•••	13.4	13.45	13.5	13.5	13.5	13.55	•••	•••	•••	•••	•••	10.6(*P*)	12.8	12.8(*s*)	12.8
•••	•••	•••	14.0	14.05	14.1	14.15	14.2	14.15	12.2	12.3(*s*)	12.3	12.3	12.3(*s*)	12.3	•••	•••	•••
•••	•••	•••	15.5	15.5	15.6	15.8	15.8	15.9	•••	•••	•••	•••	•••	•••	13.1	13.1	13.15
•••	•••	•••	•••	•••	16.0	•••	•••	•••	13.25	13.2	13.2	13.2	13.2	13.25	•••	•••	•••
•••	•••	•••	17.0	17.0	16.8	17.0	17.0	16.9	•••	•••	•••	•••	•••	•••	13.75	13.75	13.8
•••	•••	•••	22.0	22.0	22.0	22.8	22.8	22.6	13.85	13.8	13.8	13.8	13.8	13.9	•••	•••	•••
•••	•••	•••	•••	•••	•••	•••	•••	•••	•••	•••	•••	•••	•••	•••	15.75	15.75	15.8
•••	•••	•••	•••	•••	•••	•••	•••	•••	15.6	15.6	15.6	15.8	15.6	15.55	•••	•••	•••
•••	•••	•••	•••	•••	•••	•••	•••	•••	16.8	16.6	16.6	16.6	16.7	16.6	•••	•••	•••
•••	•••	•••	•••	•••	•••	•••	•••	•••	•••	•••	•••	17.1	17.3	17.2	•••	•••	•••
•••	•••	•••	•••	•••	•••	•••	•••	•••	•••	•••	•••	22.8	22.8	22.5	•••	•••	•••

TABLE IV. Energies (in eV) of prominent features in the reflectance spectra of BeO and MgO.

400 K	300 K	100 K	400 K	300 K	100 K	400 K	300 K	100 K
	BeO $\vec{E}\parallel\vec{c}$			BeO $\vec{E}\perp\vec{c}$			MgO	
10.2	10.3	10.35	10.25	10.28	10.35	7.45	7.55	7.65
•••	10.42	10.52	•••	10.45	10.55	•••	•••	7.7
10.9	11.3(*s*)	11.2	•••	•••	•••	•••	9.8(*s*)	9.8
12.85	12.8	12.95	12.8	12.8	12.8	10.9	11.0	11.0
14.45	14.3(*s*)	14.45	14.0	14.0(*s*)	14.0(*s*)	13.4	13.45	13.45
17.4	17.4(*s*)	17.45	17.8	18.0(*s*)	18.0	14.6	14.8	14.8
18.5	18.5	18.55	•••	•••	•••	17.6	17.6	17.65
20.0	20.0	20.0	20.0	20.0	20.0	18.4	18.6	18.6
25.0	25.0(*s*)	25.25	26.0	26.0(*s*)	26.0	19.35	19.5	19.4
•••	•••	•••	•••	•••	•••	21.0	21.2	21.2
•••	•••	•••	•••	•••	•••	24.2(*s*)	24.5(*s*)	24.6(*P*)

pseudopotential method. They then calculated the joint density-of-states[11,24,25,40,43] and matrix elements, and thereby obtained a theoretical ϵ_2 curve, from which a reflectance spectrum was obtained by a Kramers–Kronig inversion. We shall compare these theoretical reflectance and ϵ_2 curves with those from our experiment. The method used in obtaining the experimental ϵ_2 curves will be presented in the section dealing with Kramers–Kronig inversion (Sec. VII).

Figures 14 and 15 show both theoretical[11] and experimental curves for the reflectance and ϵ_2 of ZnS. The theoretical curves were calculated for a ZB crystal while the experimental sample was WU. This comparison is valid since little anisotropy has been observed, and the experimental spectrum for ZB ZnS is similar to spectra for hexagonal ZnS for either polarization. Perhaps the most important and general comment to be made on these figures is that the theoretical curves underestimate the oscillator strength at low energies and overestimate it for higher energies. Note also that the agreement for the energy of structures is fairly good for $E < 8$ eV, but there may be disagreement of more than 1 eV at higher energies. Finally, note that the theoretical curves neglect structure due to the *d* states of the Zn.

Our sample of ZnSe was in the zinc-blende structure. It was measured only at 300 and 100 K (as shown in Fig. 16). The surface was therefore not heated to 400 K to remove adsorbed gases; we judge this to be a minor effect. Our agreement

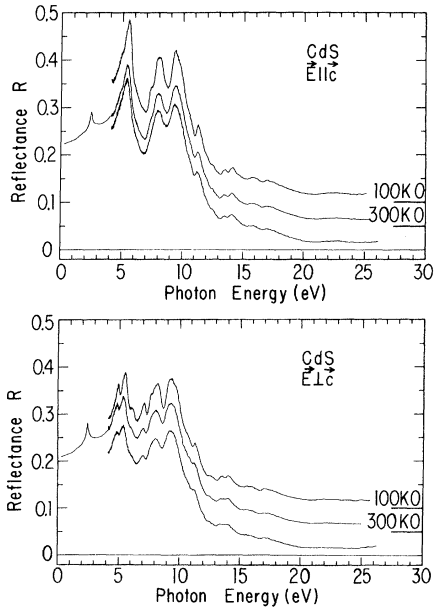

FIG. 23. Reflectance spectra of CdS $\vec{E}\perp\vec{c}$ and $\vec{E}\parallel\vec{c}$, $RS = 0.05$.

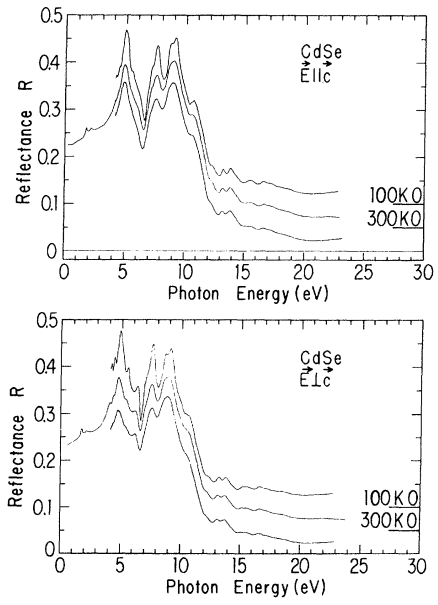

FIG. 24. Reflectance spectra of CdSe $\vec{E}\perp\vec{c}$ and $\vec{E}\parallel\vec{c}$, $RS = 0.05$.

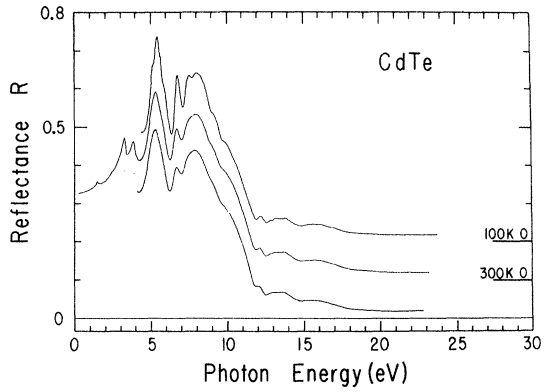

FIG. 25. Reflectance spectra of CdTe, $RS = 0.1$.

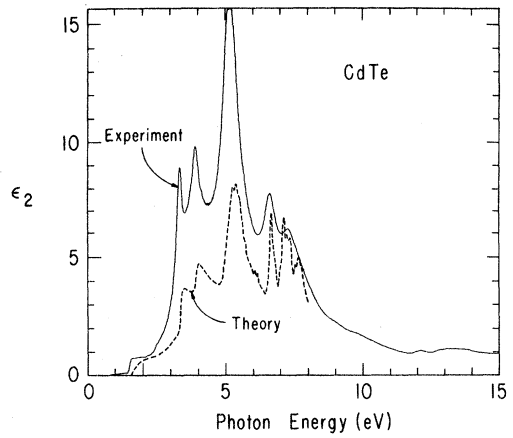

FIG. 27. Same as Fig. 15 for CdTe. The theoretical curve is from Ref. 25.

with the 300-K experimental results of Petroff and Balkanski[24] is not nearly as good as with the theoretical calculations of Walters and Cohen in the same paper. The experimental agreement is better at low temperatures. The 6.5-eV peak measured by Petroff and Balkanski at 15 K looks much like our 100-K results except for a shoulder on the low-energy side not seen in our measurements.

Figures 17 and 18 compare the experimental and theoretical[24] curves for the reflectance and ϵ_2 of ZnSe. We again note the low computed oscillator strength at low energies, and the too large oscillator strength at higher energies. In this instance, the calculated position of structures is in relatively good agreement up to about 10 eV; the small calculated peak at about 7 eV is indeed a well-defined peak at 90 K (see Fig. 17), although not so well separated from the main peak.

Figure 19 shows our measurements on ZnTe. Again our measurements are in disagreement with those of Petroff and Balkanski[24]; our magnitudes are higher by $\Delta R = 0.1$, and we observe more structure at energies above 7.6 eV. In their measurements at 15 K they observed two shoulders on the low-energy side of the 5.5-eV peak; these shoulders were not seen at 90 K in our measurements. Note the well-defined doublet at about 3.5 eV; this again is SO splitting, which is larger in tellurium than in selenium. Again the 100-K measurement reveals no new structure; however, the peak at 7 eV shows marked temperature dependence, as was also seen for the corresponding structure in ZnSe (8.5 eV) and ZnS (9.5 eV).

Figures 20 and 21 show comparisons of theoretical[24] and experimental curves for ZnTe. Although the calculated higher-energy reflectance is higher than that observed experimentally, the reverse is true for ϵ_2; the experimental ϵ_2 is larger than the theoretical ϵ_2 for $E < 8$ eV. The basic experimental curve is the reflectance, while ϵ_2 is the principal calculated quantity. The comparison between theory and experiment therefore requires a Kramers–Kronig inversion of one or the other of the basic curves. We believe that the experimental curve should be analyzed in this instance for two related reasons. The first reason is that the experimental data cover a wider energy range than do the density-of-states calculations. The second reason is also a result of the large energy range covered by the experimental data; we observe transitions from the zinc-3*d* and tellurium-5*s* states, which are not included in the density-of-states calculations. The neglect of outer core states of course would affect the calculated ϵ_2 at energies

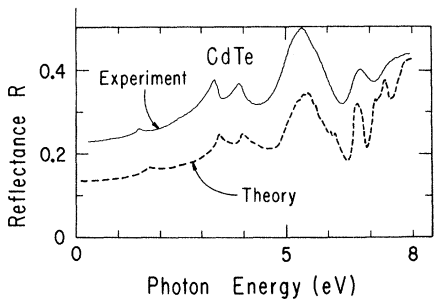

FIG. 26. Same as Fig. 14 for CdTe. The theoretical curve is from Ref. 25.

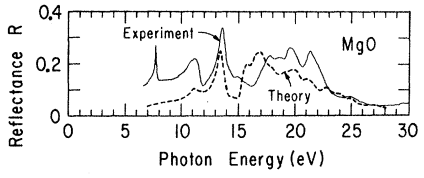

FIG. 28. Same as Fig. 14 for MgO. The theoretical curve is from Ref. 43.

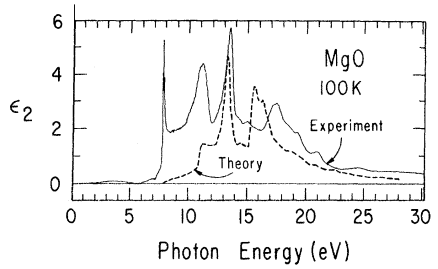

FIG. 29. Same as Fig. 15 for MgO. The theoretical curve is from Ref. 43.

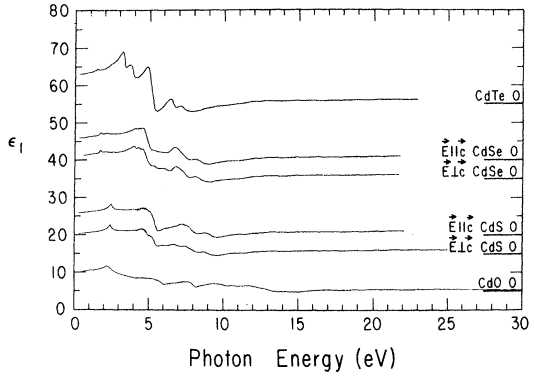

FIG. 31. Same as Fig. 30 for cadmium compounds.

for which core-state transitions are allowed. It would also affect the extrapolation required to compute a reflectance from this calculated ϵ_2.

Proceeding to the Cd series, we see in Fig. 22 the temperature dependence of the CdO spectra. As in ZnO, there is very little temperature dependence. In CdS (Fig. 23) there is both temperature dependence and some anisotropy. The first peak (C) above the band-gap exciton is a doublet for $\vec{E}\perp\vec{c}$, but only one peak is seen for $\vec{E}\|\vec{c}$. This has been explained[28,40] as a crystal-field splitting of the peak labeled C in our notation, or E_1 in the notation of Cardona. As explained in Sec. III, this is caused by transitions along the Λ axis in ZB materials. The WU crystal field splits this into states along Γ-A and states along U; these states have different energies in CdS, leading to this doublet. Selection rules forbid the transitions at Γ for $\vec{E}\|\vec{c}$, leading to only one peak in that polarization. Our measurements in general agree well with those of Cardona,[28] although his reflectance magnitudes are slightly higher than ours. In addition, at energies above 8 eV there are some differences in the shape of peaks, and he did not observe the doublet at 13.5 eV.

Figure 24 shows our measurements upon CdSe for $\vec{E}\perp\vec{c}$ and $\vec{E}\|\vec{c}$. The latter measurement contains a major discrepancy with earlier work. Both Cardona and Harbeke[28] and Hengehold and Fraime[50] found three peaks of about the same magnitude for the peak labeled C in this paper. Cardona measured a polished and etched crystal. Hengehold measured as-grown platelets. Our measurements were performed on two cleaved single crystals, one sample purchased from Semi-Elements, the other kindly denoted by Reynolds of the Aerospace Research Laboratories. In both cases the C peak consisted of one major peak (E_1B in Cardona's notation) with a low-energy shoulder and a slight peak at still lower energies ($E_1A_{1,2}$ in Cardona's notation). We do not believe this is due to poor polarization of our incident radiation, as we did see a well-defined polarization dependence in a similar energy range for CdS. This discrepancy with earlier work is not yet understood. Another disagreement with Cardona's results lies in the peak at 6 eV; we observe this peak only in $\vec{E}\perp\vec{c}$, he sees it (labeled E_0') at $\vec{E}\|\vec{c}$ only.[28] At higher energies we note that the peak at 9 eV becomes two distinct structures upon cooling to 90 K; no other new structures are observed at 100 K.

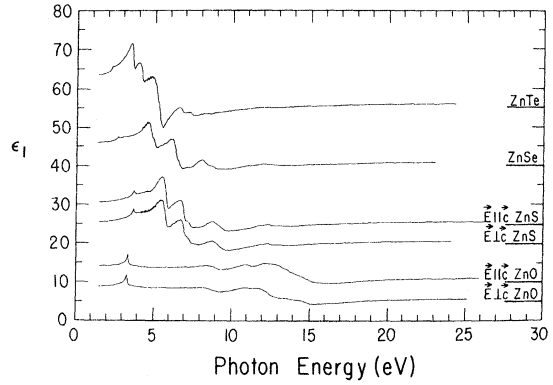

FIG. 30. Experimental ϵ_1 spectra for the zinc compounds. The curves were vertically shifted as indicated to prevent overlap.

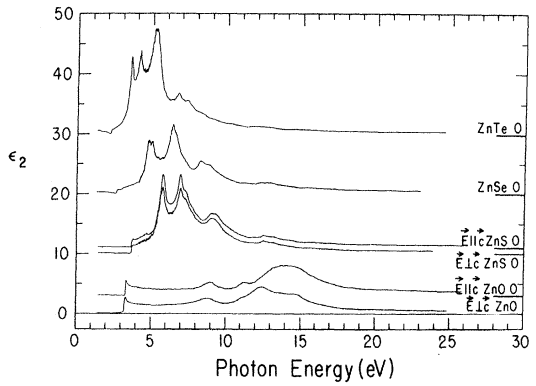

FIG. 32. Experimental ϵ_2 spectra for the zinc compounds. The curves were vertically shifted as indicated to prevent overlap.

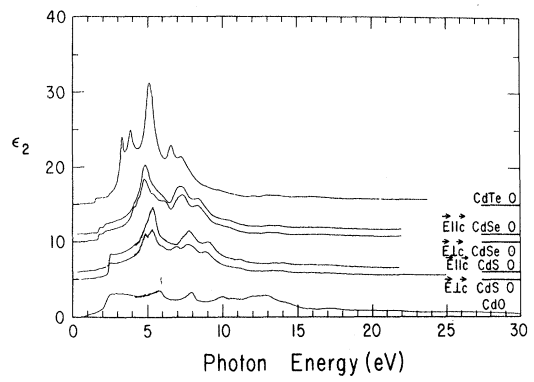

FIG. 33. Same as Fig. 32 for the cadmium compounds.

Figure 25 shows our results for CdTe. This sample was ZB. Our data agree well with earlier low-temperature measurements[25] as to the positions of reflectance structure, but our magnitudes are very different; our measurements yield $R = 0.5$ at 8 eV, in contrast with the reported value $R = 0.35$ for the same peak. Once again (as in CdSe) the last VB peak split into two structures upon cooling. In this material we also see shoulders on the 5-eV peak which were not seen at room temperature.

Figures 26 and 27 compare the calculated[25] and experimental curves for CdTe. We again note the low theoretical curve for low energies and note also (as in ZnTe) that the theoretical curve exceeds the experimental curve only at rare intervals. We again believe that this is due to the neglect of outer core states, which may make some contribution due to the breakdown of selection rules.

The small calculated oscillator strength at low energies is perhaps due to the neglect of electron-hole interactions; the too large oscillator strength at higher energies (but where core states do not contribute) would also be due to this neglect, as the electron-hole interactions can only redistribute oscillator strengths within the constraints imposed by the f-sum rule.

If we now look at Figs. 28 and 29 we may compare experimental and theoretical[43] reflectance and ϵ_2 spectra for MgO. The experimental curves are for 100-K sample temperature; we thus see the doublet at the band-gap exciton. This doublet is apparently due to a phonon-exciton complex[60,61] of some sort; the theory[62,63] of this structure is still in a state of flux. Note once again that there is very little calculated oscillator strength associated with the first transition above the band gap (at 11 eV) as compared with the experimental value. This peak shows little temperature dependence. We have measured a polished sample of MgO. The band-gap exciton was very broad and temperature independent in the polished sample, but the 11-eV peak was not changed in shape or position.

The spectra for BeO were presented in Fig. 9. The band-gap exciton is a doublet, presumably due to the phonon-exciton complex,[61] which is very temperature dependent. All other structures change little in the temperature range 400–100 K.

VII. KRAMERS–KRONIG ANALYSIS

The Kramers–Kronig relations for normal-incidence reflectance were applied to the room-temperature near-normal-incidence reflectance spectra presented in this paper. We have therefore calculated n, k, ϵ_1, ϵ_2, and $-\mathrm{Im}1/\epsilon$ and have integrated $\omega\epsilon_2$ to obtain $N_{\mathrm{eff}}(E)$, the effective number of electrons contributing to the absorption at energies less than E.

The primary difficulty in a Kramers–Kronig analysis of any reflectance measurement lies in the requirement of measurements for all energies $0 < E < \infty$; this is obviously impossible to achieve experimentally, and therefore approximations are required. For the purposes of analyzing the materials reported here, the following simple form for the high-energy extrapolation was found to be quite

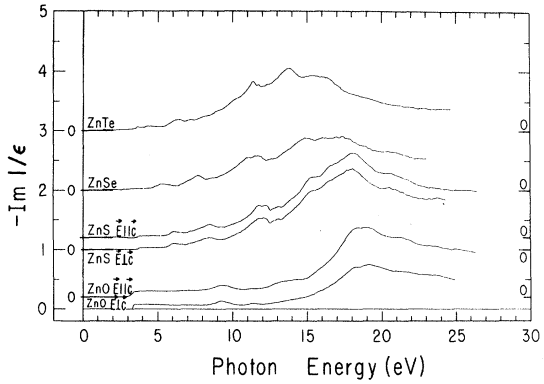

FIG. 34. Experimental $-\mathrm{Im}(1/\epsilon)$ spectra for the zinc compounds. The curves were zero shifted as indicated to prevent overlap.

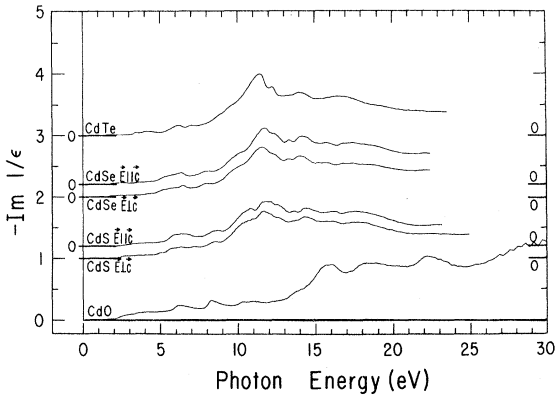

FIG. 35. Same as Fig. 34 for the cadmium compounds.

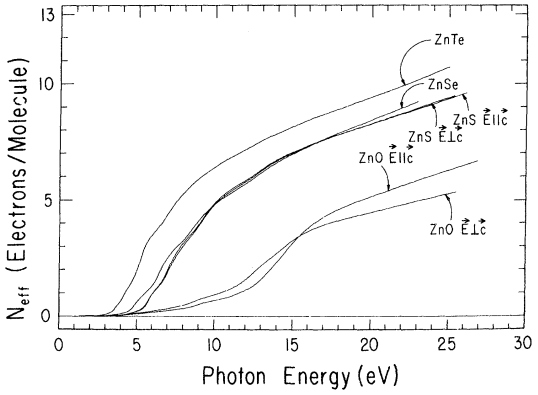

FIG. 36. Effective number of electrons per molecule contributing to the absorption at energies less than E for the zinc compounds.

adequate: $R(E)=R(E_b)(E_b/E)^x$ $E>E_b$, where E_b is the highest energy for which the reflectance of the sample was obtained, and x is a parameter varied so as to give the proper values for k and ϵ_2 in the region below the fundamental absorption edge (x typically was approximately 2). The low-energy extrapolation is obtained by smoothly fitting our reflectance value at 0.6 eV to the reported ϵ_∞. Far more elaborate procedures for performing a Kramers–Kronig analysis with data from a limited energy range have been proposed,[64–66] but seem to be unnecessary for these materials, perhaps because of our large energy range. For materials in which our reflectance spectra were similar to those reported elsewhere (e.g., CdS by Cardona),[30] ϵ_1 and ϵ_2 as reported and as obtained by our analysis were also similar. Further, our computed energy-loss measurements agree quite well with the measurements of electron energy loss reported recently.[67–70] Finally, our results for N_{eff} (25 eV) are quite reasonable in terms of our understanding of these materials. Since the high-energy approximation affects this result rather strongly and was chosen with no knowledge of N_{eff} (25 eV), this is indeed a test of this extrapolation.

Figures 30–37 show our curves for ϵ_1, ϵ_2, $-\mathrm{Im}1/\epsilon$, and $N_{eff}(E)$ for the Zn and Cd series. The curves for ϵ_1 and ϵ_2 will not be discussed separately from the reflectance spectra they were derived from. The $-\mathrm{Im}1/\epsilon$ are equivalent to electron-energy-loss curves within the random-phase approximation. The curves we calculate agree quite well with reported measurements of electron energy loss (see Table V).

We shall use the results of our calculations $N_{eff}(E)$ to further discuss the question of absolute magnitudes, a subject of considerable controversy in this energy range (see Sec. VI for a close comparison of the currently proposed magnitudes with those obtained by other workers). Very few workers have published a value for $N_{eff}(E)$. One of the cases in which it has been presented is the work of Klucker *et al.*[33] upon ZnO. Although our magnitudes agree quite well at the band-gap exciton they obtained a reflectance about two-thirds the reflectance reported here for the peak at 15 eV. For this reason, they did not find as large an oscillator strength for this peak as reported in the present work (see Fig. 38). Figure 36 shows the results of our calculations of $N_{eff}(E)$ for the zinc compounds. Note that in ZnO $\vec{E}\parallel\vec{c}$, N_{eff} (25 eV) is about 6.4 electrons per molecule, which corresponds to nearly exhausting the six valence-band electrons and beginning the absorption due to the Zn -3*d* and the oxygen-2*s* states. The results for ZnO $\vec{E}\perp\vec{c}$ are not so well defined. Our measurements on ZnO in the energy range 1–4.1 eV have shown almost no anisotropy at 4.1 eV, in contrast to the $\Delta R=0.02$ (for $R=0.12$) reported by Klucker *et al.*[33] Our measurements on this material in the high-energy apparatus have on various occasions indicated an anisotropy at 4.1 eV, while other measurements did not reveal such a difference in re-

TABLE V. N_{eff} at 25 eV from the data of this work and 36 eV to E_b from Ref. 71.

Material		N_{eff} at energy (eV)		N_{eff} $(36-E_b)$[a]	E_b (eV)	N_{eff} (total)
ZnO	$\vec{E}\parallel\vec{c}$	6.2	26			
	$\vec{E}\perp\vec{c}$	5.2	25			
ZnS	$\vec{E}\parallel\vec{c}$	9.5	26			
				7.2	92	16.5
	$\vec{E}\perp\vec{c}$	9.1	24			
ZnSe[b]		9.2	23	10.4	120	19.6
ZnTe[b]		10.4	24	18	89	28.4
CdO		6.3	30			
CdS	$\vec{E}\parallel\vec{c}$	9.3	22			
				6.2	60	15.3
	$\vec{E}\perp\vec{c}$	8.9	25			
CdSe[b]	$\vec{E}\parallel\vec{c}$	9.6	22			
				11.5	70	21.2
	$\vec{E}\perp\vec{c}$	10.0	22			
CdTe[b]		13.0	23	26.5	90	39.4

[a]Reference 71.

[b]High energy N_{eff} includes core states of chalcogen.

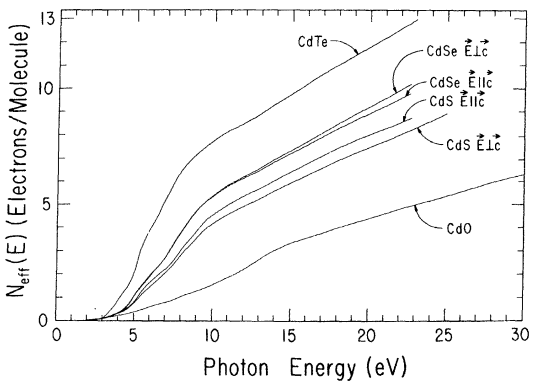

FIG. 37. Same as Fig. 36 for the cadmium compounds.

TABLE VI. Energies of peaks in $-\mathrm{Im}\,(1/\epsilon)$ compared with electron-energy-loss measurements.

Material	Energies (eV)											
ZnO $\vec{E}\parallel\vec{c}$	3.35	9.25	11.4			18.2, 19.1	21.5		23.8	25.0		
$\vec{E}\perp\vec{c}$	3.3	9.3	11.2		13.6	18–19	21.4		23.5	25.0		
Ref. a		9.3	11.15		13.5	18.9	21.8		23			
Ref. b	4.4	8.6, 9.3			13.1	17.8						
ZnS $\vec{E}\parallel\vec{c}$	6.0	7.0	8.4		11.8, 12.2	13.0	14.0(*s*) 15.3		18.0	20.6		
$\vec{E}\perp\vec{c}$	6.0	7.0	8.5				15.3		18.0	20.5	23.5	
Ref. a	6.2		8.1		11.7		15.1		17.5			
Ref. b	6.2		8.3		11.7		14.3		18.0		24.4	
ZnSe	5.05	7.65	10.9		11.6	14.8	16		17.5	20.5		
Ref. a	5.3	7.2		11.5		14.9		16.9				
Ref. b	5.6	7.9		11.4		13.7		17.1		20.6	24.1	
ZnTe	4.2	6.3	7.2		8.0(*s*)	10.0(*s*)	11.35		13.8	15.3	16.4(*s*)	
Ref. a	4.1	6.2					11.2		13.9	15.3		
Ref. b	4.5	6.6				10.4	12.4			15.5		26.0
CdO	6.1	8.3	10.2		11.0	13.8(*s*)		15.8	18–19	22	30	
Ref. c	6.6	8.6		10.9				15.8	17.8	22.6	30.6	35.5
CdS $\vec{E}\parallel\vec{c}$	5.6	6.5	8.7		10.8(*s*)	11.8		12.6(*s*)	13.6	14.4	16	18
$\vec{E}\perp\vec{c}$	5.6	6.5	8.6		10.4(*s*)	11.6		12.6(*s*)		14.3	16	17.5
Ref. a	6.2		8.4				12.1			14.5		17.7
REEL[d]	6.8					11.2				14.4		18.2
TEEL[d]	6.9							12.6		14.9	16.7	18.6
CdSe $\vec{E}\parallel\vec{c}$	6.4	8	9.8(*s*)		11.8	12.4		13.3	14.2	15.8	16.8–17	
$\vec{E}\perp\vec{c}$	6.5	8	9.8(*s*)		11.6	12.5(*s*)		13.3	14.0	15–16	16.8–17.4	
Ref. a	5.7				11.9				14.2		17.2	
REEL[d]	6.4		10.7					13.8			17.6	
CdTe	3.4	4	6.2		7	8(*s*)		11.4	12.2	14	16.5	
REEL[d]		4.5	6.5			9.6		10.7		13.6	16.1	22.5
TEEL[d]		4.2	6.1			8.8		11.8		14.1	16.4	22.4

[a]Reflection electron energy loss, Ref. 67.
[b]Reflected electron energy loss, Ref. 68.
[c]Reflected electron energy loss, Ref. 70.
[d]Reflected electron energy loss and transmitted electron energy loss, Ref. 69.

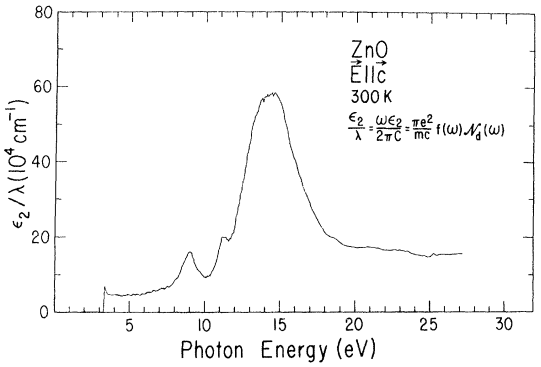

FIG. 38. Oscillator strength for ZnO $\vec{E} \parallel \vec{c}$.

flectance for the two polarizations. Using the high-energy data for $\vec{E} \perp \vec{c}$, which agreed with our reflectance data in the visible spectral region, we obtain N_{eff} (25 eV) = 5.3 electrons per molecule. If we use the high-energy data indicating anisotropic reflectance at 4.1 eV and use the data below 4 eV reported by Klucker *et al.*,[33] we obtain N_{eff} (25 eV) = 5.8 electrons per molecule. We are uncertain which value to take. Further work is required to determine the correct values and to discover the reason for this variance. Klucker *et al.*[33] obtain about 4 electrons per molecule, which is too low—presumably because of their low reflectance magnitude at the 15-eV peak.

Figure 37 shows a plot of $N_{eff}(E)$ for the cadmium series. Note that in both the Zn and the Cd series the oxides have a low $N_{eff}(E)$ for $E < 10$ eV, although by 25 eV they approach or exceed 6 electrons per molecule. In the chalcogenides, N_{eff} is higher and attains a higher final value. This corresponds to more absorption by the d shell of the metal and the s shell of the chalcogens.

There have been some soft-x-ray absorption measurements (36–150 eV) on evaporated thin films of the Zn and Cd chalcogenides by Cardona and Haensel.[71] They performed a modified-sum-rule calculation on their results, assuming the real part of the index of refraction n was unity, an assumption presumably valid to within 10%. The results of their calculation are shown along with our results in Table VI, where those materials having core states too tightly bound to be observed in our measurements but occurring at energies $E < 80$ eV, are indicated with an asterisk. Combining their results with ours, we can obtain an N_{eff} (80 eV) if we neglect the energy range 25–36 eV. This energy range should contribute little to the sum rule because of the process sometimes called the delayed d threshold,[72] so the error in ignoring this energy range should not be much more than two electrons. This is barely outside the errors of the calculation of N_{eff} ($\pm$ 10%) and hence perhaps should be ignored. However, an examination of N_{eff} (E max) for ZnS and CdS shows that we are consistently low (below the expected 18) by an average of 2.1 electrons per molecule, and perhaps all the other results should be corrected by this amount.

The accuracy of a Kramers–Kronig analysis is difficult to discuss. We present here a brief discussion of our estimate of the uncertainties in $N_{eff}(E)$, as it provides a single number to discuss. There are two obvious sources of error: the extrapolation and the reflectance errors. All extrapolations that meet our criterion of causing k and ϵ_2 to be close to zero for energies below the fundamental absorption region leads to values of $N_{eff}(E)$ within 5% of one another for the same reflectance data. The reproducibility of our reflectance data is perhaps indicated by the differences in $N_{eff}(E)$ for the two polarizations of an anisotropic material. We report on four such materials: CdS, CdSe, ZnO, and ZnS. We believe that the difference between $N_{eff}(E)$ for $\vec{E} \perp \vec{c}$ and $\vec{E} \parallel \vec{c}$ for CdS, CdSe, and ZnS provides a good indication of the accuracy of these values. We believe a similar level of accuracy holds for ZnSe, ZnTe, and CdTe, since they offered similar reproducibility. As stated earlier, our results for ZnO were not consistent; we therefore do not have the same confidence in the results for ZnO $\vec{E} \perp \vec{c}$ as for the zinc and cadmium chalcogenides. Finally, our reflectance spectra for CdO required a large scale factor because of the curved sample surface; the values for CdO are therefore also less reliable than for the chalcogenides.

VIII. CONCLUSION

Synchrotron radiation has made it possible to extend the previous energy limits of our knowledge of the temperature and polarization dependence of the optical constants of the II-VI compounds reported here. These more detailed high-photon-energy measurements have also facilitated the study of the outer core states of these materials, providing much information as to the energy position and width of these states in the solid.

The Penn–Phillips average energy gap was found to be a scaling parameter for interband transition energies. It was found to be useful in interpreting the spectra of CdO and ZnO, the least studied of the IIB-VI compounds.

ACKNOWLEDGMENTS

I wish to thank the following people for graciously giving the samples reported upon here: S. B. Austerman of Autonetics for BeO, G. Heiland of Techn. Hochschule Aachen for ZnO, F. T. Smith of Lincoln Laboratories for CdO, K. W. Böer of

the University of Delaware for CdS, and D. C. Reynolds of the Aerosapce Research Laboratories for ZnS, ZnTe, CdSe, and CdTe. I am indebted to H. Fritzsche for his guidance, his many insights, and his enthusiastic support during all phases of this work. I am also very grateful to K. Murase and J. W. Osmun for their valuable cooperation and assistance in much of this research, and to G. W. Rubloff and U. Gerhardt for this contributions in the early stages of this project. I thank S. J. Hudgens for a critical reading of the manuscript. I also thank J. C. Phillips, R. L. Hengehold, and T. Bergstresser for enlightening discussions about this work. Finally, it is a pleasure to acknowledge the cooperation and encouragement of the staff of the University of Wisconsin Physical Science Laboratory, especially E. M. Rowe, C. H. Pruett, R. Otte, and N. Lien.

*Research sponsored by the Air Force Office of Scientific Research, Office of Aerospace Research, USAF, under Contract Nos. F44620-71-C-0025 and F44620-70-C-0029. We have also benefited from support of Materials Sciences by the Advanced Research Projects Agency at The University of Chicago.

†Submitted in partial fulfillment of the requirements for the Ph.D. degree at the University of Chicago.

‡Present address: Department of Engineering and Applied Physics, Harvard University, Cambridge, Mass. 02138.

[1]J. C. Phillips, Solid State Physics 18, 56 (1966).

[2]Fred H. Pollak, *International Conference on II-VI Semiconducting Compounds* (Benjamin, New York, 1967).

[3]James A. R. Samson, *Techniques of Vacuum Ultraviolet Spectroscopy* (Wiley, New York, 1967), Chap. 5.

[4]G. W. Rubloff, H. Fritzsche, U. Gerhardt, and J. Freeouf, Rev. Sci. Instr. 42, 1507 (1971).

[5]E. M. Rowe, R. A. Otte, C. H. Pruett, and J. D. Steben, IEEE Trans. Nucl. Sci. NS-16, 159 (1969).

[6]W. Lotz, J. Opt. Soc. Am. 60, 206 (1970).

[7]U. Rössler, Phys. Rev. 184, 733 (1969).

[8]R. A. Powell, W. E. Spicer, and J. C. McMenamin, Phys. Rev. Letters 27, 97 (1971).

[9]J. Freeouf, H. Fritzsche, K. Murase, and J. W. Osmun (unpublished).

[10]R. N. Euwema, T. C. Collins, D. G. Shankland, and J. S. DeWitt, Phys. Rev. 162, 710 (1967).

[11]J. P. Walter and M. L. Cohen, Phys. Rev. 183, 763 (1969).

[12]J. C. Phillips, Rev. Mod. Phys. 42, 317 (1970).

[13]J. A. Van Vechten, Phys. Rev. 182, 891 (1969).

[14]M. L. Cohen, P. J. Lin, D. M. Roessler, and W. C. Walker, Phys. Rev. 155, 992 (1967).

[15]M. Altwein, H. Finkenrath, C. Konak, J. Stuke, and G. Zimmerer, Phys. Stat. Sol. 29, 203 (1968).

[16]E. Loh, Solid State Comm. 2, 269 (1964).

[17]D. G. Thomas and J. J. Hopfield, Phys. Rev. 116, 573 (1959).

[18]M. Cordona, J. Appl. Phys. 32, 2151 (1961).

[19]R. G. Wheeler and J. O. Dimmock, Phys. Rev. 125, 1805 (1962).

[20]M. Cardona and G. Harbeke, Phys. Rev. Letters 8, 90 (1962).

[21]D. T. F. Marple and H. Ehrenreich, Phys. Rev. Letters 8, 87 (1962).

[22]M. Cardona, K. L. Shaklee, and F. H. Pollak, Phys. Rev. 154, 696 (1967).

[23]Y. Petroff, M. Balkanski, J. P. Walter, and M. L. Cohen, Solid State Comm. 7, 459 (1969).

[24]J. P. Walter, M. L. Cohen, Y. Petroff, and M. Balkanski, Phys. Rev. B 1, 2661 (1970).

[25]D. J. Chadi, J. P. Walter, M. L. Cohen, Y. Petroff, and M. Balkanski, Phys. Rev. B 5, 3058 (1972).

[26]M. Balkanski and Y. Petroff, in *Proceedings of the Seventh International Conference on the Physics of Semiconductors* (Academic, New York, 1964), p. 245.

[27]M. Cardona and D. L. Greenaway, Phys. Rev. 131, 98 (1963).

[28]M. Cardona and G. Harbeke, Phys. Rev. 137, A1467 (1965).

[29]M. Aven, D. T. F. Marple, and B. Segall, J. Appl. Phys. 32, 2261 (1961).

[30]M. Cardona, M. Weinstein, and G. A. Wolff, Phys. Rev. 140, A633 (1965).

[31]W. C. Walker and J. Osantowski, J. Phys. Chem. Solids 25, 778 (1964).

[32]R. L. Hengehold, R. J. Almassy, and F. L. Pedrotti, Phys. Rev. B 1, 4784 (1970).

[33]R. Klucker, H. Nelkowski, Y. S. Park, M. Skibowski, and T. S. Wagner, Phys. Stat. Sol. (b) 45, 265 (1971).

[34]D. M. Roessler and W. C. Walker, Phys. Rev. 159, 733 (1967).

[35]C. E. Moore, *Atomic Energy Levels*, NBS Circ. No. 467 (U. S. GPO, Washington, D.C., 1949), Vols. 1–3.

[36]K. Siegbahn *et al.*, *ESCA Atomic, Molecular, and Solid State Structure Studied by Means of Electron Spectroscopy* (Almqvist and Wiksells, Uppsala, Sweden, 1967), p. 79.

[37]J. P. Walter and M. L. Cohen, Phys. Rev. B 4, 1877 (1971).

[38]Y. Onodera, M. Okazaki, and T. Inui, J. Phys. Soc. Japan 21, 2229 (1966).

[39]J. L. Birman, Phys. Rev. 115, 1493 (1959).

[40]T. K. Bergstresser and M. L. Cohen, Phys. Rev. 164, 1069 (1967).

[41]G. F. Koster, Solid State Physics 5, 173 (1957).

[42]R. H. Parmenter, Phys. Rev. 100, 573 (1955).

[43]C. Y. Fong, W. Saslow, and M. L. Cohen, Phys. Rev. 168, 992 (1968).

[44]D. J. Stukel, R. N. Euwema, T. C. Collins, F. Herman, and R. L. Kortum, Phys. Rev. 179, 740 (1969).

[45]K. Maschke and U. Rössler, Phys. Stat. Sol. 28, 577 (1968).

[46]C. Vesely and D. Langer, Phys. Rev. B 4, 451 (1971).

[47]U. Gerhardt and G. W. Rubloff, Appl. Optics 8, 305 (1969).

[48]M. L. Cohen and T. K. Bergstresser, Phys. Rev. 141, 789 (1966).

[49]S. Bloom and T. K. Bergstresser, Solid State Comm. 6, 465 (1968).

[50]R. L. Hengehold and C. R. Fraime, Phys. Rev. 174, 808 (1968).

[51]R. E. Drews, E. A. Davis, and A. G. Leiga, Phys. Rev. Letters 18, 1194 (1967).

[52]F. Herman and S. Skillman, *Atomic Structure Calculations* (Prentice Hall, Englewood Cliffs, N. J., 1963), pp. 2–9.
[53]J. L. Shay, W. E. Spicer, and F. Herman, Phys. Rev. Letters 18, 649 (1967).
[54]J. L. Shay and W. E. Spicer, Phys. Rev. 161, 799 (1967).
[55]J. L. Shay and W. E. Spicer, Phys. Rev. 169, 650 (1968).
[56]C. J. Vesely, R. L. Hengehold, and D. W. Langer, Phys. Rev. B 5, 2296 (1972).
[57]F. Herman and S. Skillman, *Atomic Structure Calculations* (Prentice Hall, Englewood Cliffs, N. J., 1963), pp. 2–7.
[58]D. Eastman (private communication).
[59]Y. S. Park and J. R. Schneider, J. Appl. Phys. 39, 3049 (1968).
[60]W. Y. Liang and A. D. Yoffe, Phys. Rev. Letters 20, 59 (1968).
[61]W. C. Walker, D. M. Roessler, and E. Loh, Phys. Rev. Letters 20, 847 (1968).
[62]Y. Toyozawa and J. Hermanson, Phys. Rev. Letters 21, 1637 (1968).
[63]J. Sak, Phys. Rev. Letters 25, 1654 (1970).
[64]D. M. Roessler, Brit. J. Appl. Phys. 17, 1313 (1966).
[65]P. O. Nilsson and L. Munkby, Phys. Kondens. Materie. 10, 290 (1969).
[66]R. K. Ahrenkiel, J. Opt. Soc. Am. 61, 1651 (1971).
[67]T. Tomoda and M. Mannami, J. Phys. Soc. Japan 27, 1204 (1969).
[68]R. L. Hengehold and F. L. Pedrotti, Bull. Am. Phys. Soc. 17, 271 (1972).
[69]R. L. Hengehold and F. L. Pedrotti, Phys. Rev. B 6, 2262 (1972).
[70]R. L. Hengehold and F. L. Pedrotti (private communication).
[71]M. Cardona and R. Haensel, Phys. Rev. B 1, 2605 (1970).
[72]Delayed d threshold refers to the fact that (in atomic notation) d-p transitions occur at lower energies than d-f transitions; d-p transitions are strong near threshold and become weak quickly, while d-f transitions increase oscillator strength for a large energy range before reaching a maximum. See Ref. 71; also U. Fano and J. W. Cooper, Rev. Mod. Phys. 40, 441 (1968).

PHYSICAL REVIEW B VOLUME 7, NUMBER 8 15 APRIL 1973

Effect of Strain on the Secondary Band Extrema of PbS, PbSe, PbTe, and SnTe†

Sohrab Rabii
University of Pennsylvania, Philadelphia, Pennsylvania 19174
(Received 7 August 1972)

The energy levels associated with the secondary extrema in the energy-band structure of PbS, PbSe, and PbTe, at $\vec{k}=(\pi/a)(4/5, 4/5, 0)$, are calculated using the augmented-plane-wave method. The resulting wave functions, along with those previously calculated for SnTe, are used to obtain isotropic and uniaxial deformation potentials for all the energy levels at this point in the Brillouin zone. The results are compared with the temperature coefficients of the various gaps in the "two-band model" for the galvanomagnetic properties of these compounds. The sign of the calculated dE_g/dT and $d\Delta E_v/dT$ for the lead chalcogenides are in agreement with the experimental results. The agreement for the magnitudes, although not uniformly good for all cases, is satisfactory and presents a coherent picture for the relationship between these compounds.

I. INTRODUCTION

The existence of a "second valence band" was originally postulated to explain the temperature dependence of the galvanomagnetic properties of PbTe[1] and SnTe.[2] Subsequent experimental results appear to corroborate this assumption.[3–9] Energy-band calculations for the IV-VI compounds[10–15] have indicated the existence of a secondary set of extrema in the valence and conduction bands, in the [110] direction, that can be identified with the postulated second band. Although properly speaking these are secondary extrema in the same band, in contrast to a distinctly separate band, we shall still refer to them as "second band," because of the widespread use of this term in the literature.

The deformation potentials for the bands at point L in the Brillouin zone (main conduction and valence-band edges) for the lead salts and SnTe have already been calculated[12,15,16] from the augmented-plane-wave (APW) function with good agreement with experiment. The purpose of the present work is to calculate deformation potentials for the Σ extrema of these materials and thus furnish the information necessary to decipher the electrical and optical properties of these compounds.

The experiments in modulation spectroscopy on these compounds have furnished optical spectra, extremely rich in structure, including higher-energy optical transitions. The difficulty in deciphering such spectra is due to the fact that there are many transitions with nearly equal energy,